AIChE WILEY InterScience DISCOVER SOMETHING GREAT

Recovery of Transition Metal Complex by Reverse Flow Adsorption

Jeroen Dunnewijk, Hans Bosch, and André B. de Haan
Faculty of Science and Technology, University of Twente, 7500AE Enschede, Netherlands

DOI 10.1002/aic.11355
Published online November 13, 2007 in Wiley InterScience (www.interscience.wiley.com).

Reverse flow adsorption (RFA) is a technique with a definite potential to prevent the leaching of a homogenous catalyst. In this work, we model an RFA-process for a continuous ideally stirred tank reactor with an adsorption bed upstream and another one downstream from the reactor. The model parameters concerning adsorption equilibrium and kinetics are taken from previous experimental studies on $CoCl_2$ adsorption on polymer-bound trifenylfosfine. We use this model to study the concentration profiles of $CoCl_2$ in the adsorption beds during consecutive adsorption–desorption cycles. The model calculations show that the concentration profile eventually reaches a fixed position after a number of adsorption–desorption cycles, even though internal mass transfer was a limiting factor. Hence, the transition metal is kept within the system boundaries, which is an essential requirement for the application of RFA. © 2007 American Institute of Chemical Engineers *AIChE J,* 54: 138–142, 2008

Keywords: adsorption–desorption cycles, leaching, reverse flow, RFA-model, transition metal complex

Introduction

Homogeneous catalysts are not as common in use as heterogeneous catalysts because of difficulty of recovery. Usual recovery methods for homogeneous catalysts, including distillation and extraction, have drawbacks such as decomposition, leaching and/or the need to use additional solvents. To overcome these drawbacks, we have proposed a novel homogeneous catalyst recovery method, which combines an adsorptive separation with reverse flow technology, i.e. reverse flow adsorption (RFA).[1,2]

Reverse flow originally referred to the idea of maintaining the heat of reaction inside a fixed bed by periodically changing the flow direction.[3] Matros and Bunimovich[4] presented an extensive review of this type of application of the reverse flow reactor.

From the late eighties on, several authors[5–7] suggested using reverse flow reactors for the catalytic reduction of NO_x to contain ammonia inside a reactor. Reverse flow technology for mass entrapment to nonreactants was suggested by Beckmann and Keil.[8]

All references mentioned earlier apply to flow reversal of a *gas* phase. Reversible adsorption in the *liquid* phase, combined with Reverse flow technology, is a potential method for integrated recovery of homogeneous catalysts. To our knowledge only one research group, at the KTH in Sweden, has proposed to apply reverse flow for mass entrapment in the liquid phase. Björnbom and Hung[9–12] performed a theoretical study using flow reversal to avoid leaching of a transition metal–ligand from an imperfectly immobilized catalyst. The latter study was done for nonspecified reactants and products and focused on the mass transfer limitations of a system in which both reaction and recovery occurred in a batch reactor, assuming that decomplexation of the catalyst would not occur.

In previous work,[13,14] we proposed RFA as a method to recover a homogeneous catalyst from its liquid product solution by adsorption externally from the reactor. Hence the homogeneous catalyst system inside the reactor—e.g., the

Correspondence concerning this article should be addressed to A. B. de Haan at this current address: Dept. of Chemical Engineering and Chemistry, Eindhoven University of Technology, P.O. Box 513, 5600 MB Eindhoven, Netherlands; e-mail: a.b.dehaan@tue.nl.
Current address of J. Dunnewijk: Nijhuis Water Technology, P.O.Box 89, 7090AB Dinxperlo, Netherlands.

© 2007 American Institute of Chemical Engineers

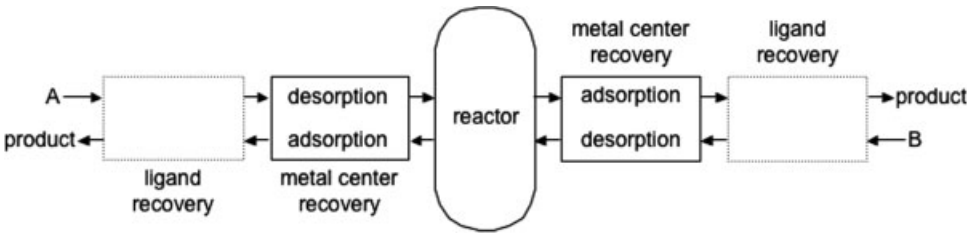

Figure 1. Homogeneous catalyst recycling by a four bed set-up of reverse flow adsorption (feed alternates between A and B).

equilibrium between the ligands and the transition metal– remains unaffected. The catalyst leaving the reactor with the product stream is recovered at process conditions by adsorption in adsorption beds downstream of the reactor (see Flow A at the right hand side in Figure 1). In the subsequent step, the direction of the process flow is reversed (Flow B in Figure 1) and the adsorption and desorption modes of the beds are interchanged.

In that work, we used $(PPh_3)CoCl_2$ as a reference transition metal catalyst and showed experimentally that it adsorbs reversibly on polymer-bound trifenylphosfine (PPh_3). The corresponding ligand may require an adsorbent with different properties. A possible set-up is shown schematically in Figure 1, where two sets of adsorbent beds are applied. In the downstream process, first the metal is adsorbed and subsequently the ligand; the reactor is fed with the same amount of fresh catalyst by desorption of both beds upstream. Before the downstream beds are saturated, the process flow is reversed.

Reversing the flow repeatedly may broaden the concentration profiles in the adsorption beds to such an extent that eventually, leaching of the catalyst may occur. The key factor in RFA is to contain the catalyst within the system. To find out if a stable process can be achieved, we developed a model describing the position of the concentration profiles of just the transition metal in both adsorption beds during adsorption and desorption as a function of time. We use this model to study whether or not the positions of these profiles at the end of subsequent cycles converge to a stable position. The kinetic and equilibrium data required by the model are deduced from kinetic experiments published previously.[15]

Dynamic Model for Concentration Gradients in an Adsorption Bed

For the calculation of just the concentration profile at the end of subsequent adsorption and desorption parts of a cycle, the use of a simplified dynamic model is appropriate. In that case, the main assumptions are[16]: isothermal operation, no channeling and constant bed porosity ε, negligible radial concentration gradients, constant velocity across the cross-section, and reversible adsorption. Furthermore, we neglect the adsorption of components other than the metal center of the catalyst, and we use an LDF-based uptake rate equation.[17,18] To minimize problems connected to numerical diffusion, we do take into account axial dispersion.

Introducing the relative concentration, $C = c/c_R$, the relative average amount adsorbed $\overline{\Gamma} = \overline{q}/q_{max}$, the relative position in the column, $Z = z/L$, and the nondimensional time $\tau = t \cdot u_0/L$, the nondimensional plug-flow model for single component isothermal adsorption in a bed homogeneously packed with single-porosity adsorbent reads as follows:

$$\varepsilon \frac{\partial C}{\partial \tau} = -\frac{\partial C}{\partial Z} + \frac{\varepsilon}{Bo}\frac{\partial^2 C}{\partial Z^2} - (1-\varepsilon)\frac{q_{max}}{c_R}\frac{\partial \overline{\Gamma}}{\partial \tau} \tag{1}$$

At Reynolds numbers of interest in this work (see Table 1), the Bodenstein number, Bo, is estimated using the correlation of Chung and Wen[20]

$$Bo \equiv \frac{u_0 L}{D_{ax}} = 0.20 \cdot \frac{L}{d_p} \text{ for } 10^{-3} < Re < 10 \tag{2}$$

with $Re \equiv \frac{u_0 d_p}{\nu}$.

The nondimensional form of the LDF uptake rate at any C and $\overline{\Gamma}$ becomes[18]

$$\frac{\partial \overline{\Gamma}}{\partial \tau} = \frac{60}{Re}\frac{D_{eff}}{\nu}\frac{L}{d_p}\left(\Gamma_i^* - \overline{\Gamma}\right) \tag{3}$$

The expression equating the LDF-uptake rate in the particles to mass flux across the stagnant film around the particles is

$$\Gamma_i^* - \overline{\Gamma} = \frac{Bi_m}{10}\frac{c_R}{q_{max}}(C - C_i) \tag{4a}$$

where the mass Biot number $Bi_m \equiv \frac{k_f d_p}{D_{eff}}$

Table 1. Parameter Values Used in the Simulations

Parameter	Protein-A on Porous Glass (from McCue et al.[19])	$CoCl_2$ on Polymer Bound (this work) PPh_3
ε	0.43	0.50
q_{max}/c_R	121	1180
$B = b\,c_R$	18.9	5.4
L/d_p	2000	$3{\cdot}10^4$
$\tau_{1/2} = t_{1/2}\,u_0/L$	–	10*
ν/D_{eff}	2.1×10^6	6.9×10^3
$Re = u_0\,d_p/\nu$	0.07; 0.14	0.22
$Bo = u_0\,L/D_{ax}$	400; 400	6.2×10^3
$Bi_m = k_f\,d_p/D_{eff}$	2.5×10^4; 3.2×10^4	$3 \times 10^{5\dagger}$

*Half cycle time in RFA.
†Chosen sufficiently high to neglect influence of external (film) diffusion.

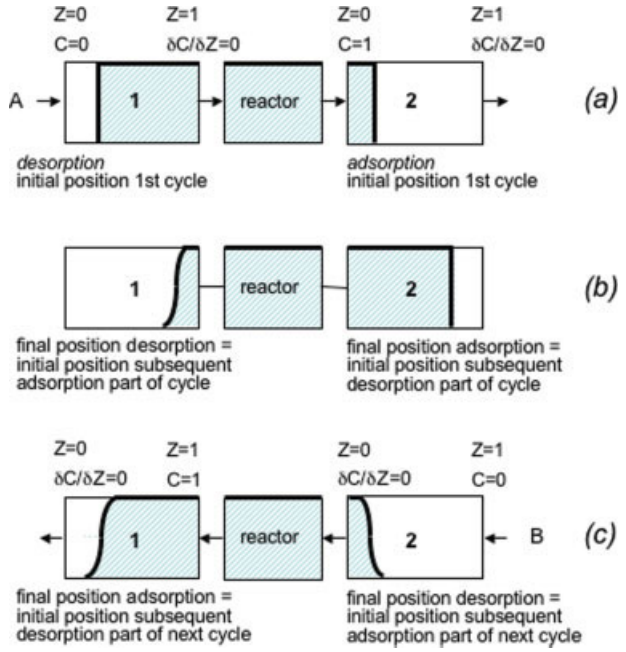

Figure 2. Concentration fronts: (a) just before, (b) halfway through, and (c) just after the first cycle as well as the definition of initial and boundary conditions (shaded area indicates adsorption zone).

[Color figure can be viewed in the online issue, which is available at www.interscience.wiley.com.]

The interface values of solid uptake Γ_i and liquid concentration C_i at any value of C and $\overline{\Gamma}$ are calculated from a Langmuir expression

$$\Gamma_i^* = \frac{B \cdot C_\mathrm{i}}{1 + B \cdot C_\mathrm{i}} \tag{4b}$$

Our simulation of a complete cycle in RFA comprises the preloading of two beds of sufficient length to ensure constant concentration at their exits as shown as shown in Figure 2a. This method of preloading the adsorption beds assures that the concentration fronts have ample space to broaden during subsequent cycles while retaining the catalyst. In the first part of a cycle, the catalyst in bed 1 is desorbed (flow A in Figure 1) and fed to the reactor while catalyst from the reactor is adsorbed in bed 2. The final position of the concentration fronts in both beds at this stage of the cycle is depicted in Figure 2b. These positions define the initial conditions at flow reversal. The final position of the fronts at the end of the first cycle is shown in Figure 2c. The initial conditions of all subsequent cycles are defined similarly. The boundary conditions of both stages in a cycle are also defined in Figure 2.

This model for a single adsorption bed (Eqs. 1–4 with initial and boundary conditions as for bed 2 in Figure 2a) has been solved in gProms (PSE, London, UK) with central differencing to calculate the change in the exit concentration as a function of time. This single bed modification has been verified with breakthrough data published by McCue et al.[19] for Reynolds numbers of 0.07 and 0.14. The parameters used are defined in Table 1. The result of this verification is shown in Figure 3. Comparison of experimental and calculated breakthrough data indicate that our LDF model describes their experimental data as well as their best model (pore diffusion).

Two-Bed Single-Component RFA-Model

Dunnewijk et al.[15] showed that external mass transfer did not limit the $CoCl_2$-uptake rate for Reynolds numbers exceeding 0.1, hence in our simulations we use $Re = 0.22$ (corresponding to one of the experimental conditions used in this reference) to neglect the influence of external mass transfer. To study the change of the concentration fronts during $CoCl_2$ recovery a two-bed form of RFA is used, as shown schematically in Figure 2. The shaded areas indicate the loaded fractions of the adsorbent beds. From the start of a cycle, a solvent flow (A in Figure 2a) is continuously fed to adsorption bed 1. $CoCl_2$ desorbs from the saturated part and is fed to the reactor. $CoCl_2$ leaving the reactor is meant to be contained within the system by adsorption in the unused fraction of adsorption bed 2. After a half cycle time $\tau_{1/2}$, the flow direction is reversed. Now bed 2 is being fed with solvent (B in Figure 2c) and the desorbing $CoCl_2$ is fed to the reactor while $CoCl_2$ leaving the reactor is adsorbed in bed 1.

The concentration of the catalysts in the reactor is constant. Thus, the choice of reactor type will not influence the simulation results. For simulation purposes, we fix the concentrations at the reactor side of both adsorption beds during adsorption:

$$Z = 1\,(\text{bed 1, adsorption}) \text{ and}$$
$$Z = 0\,(\text{bed 2, adsorption}) : C = 1 \tag{5}$$

To calculate the concentration profiles in both metal adsorption beds, the set of Eqs. 1–5, with initial and boundary conditions as in Figure 2, has been solved in g-Proms (central differencing).

Results

The results of our RFA-simulations are summarized in Figure 4. The initial position of the concentration profile in both beds is indicated by 0 in Figure 4A. During the first half of a cycle (flow a in Figure 2), $CoCl_2$ desorbs from bed 1 and is adsorbed in bed 2. The end positions halfway through a selec-

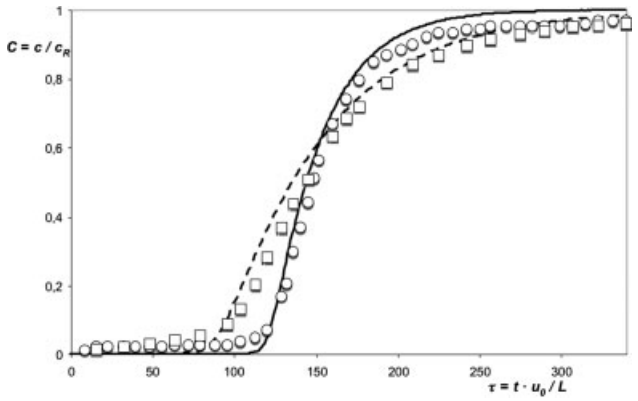

Figure 3. Single bed model calculations, experimental breakthrough data from McCue et al.[19]

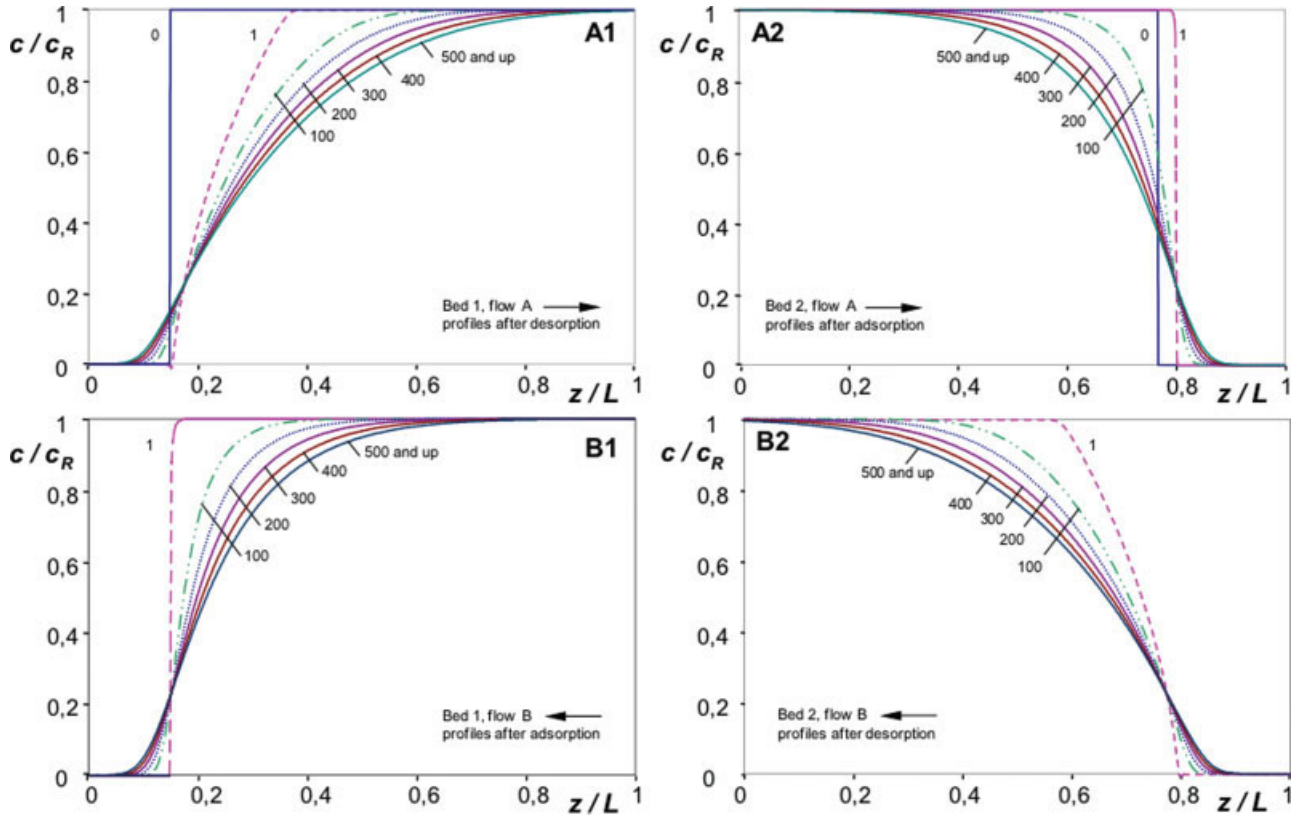

Figure 4. Concentration fronts halfway through (A1 and A2) and at the end of selected cycles (B1 and B2) 0, initial position; 1, 100, 200 etc indicate cycle number.

[Color figure can be viewed in the online issue, which is available at www.interscience.wiley.com.]

tion of cycles are shown in Figure 4A. In the second half of a cycle (flow B in Figure 2), the catalyst is desorbed from bed 2 and adsorbed in bed 1; the corresponding profiles are shown in Figure 4B.

During the first cycle, the profile in bed 1 moves from 0 to the right. Halfway through this cycle, just before reversing the flow from A to B, it reaches position 1 in Figure 4A1. Simultaneously, the profile in bed 2 (Figure 4A2) moves from position 0 to position 1. After flow reversal these profiles move back to position 1 in Figure 4B. The calculated profiles of the period halfway through cycle numbers 100, 200, and up to 500 are also shown in Figure 4A. Their positions at the end of these cycles are given in Figure 4B. Profiles calculated for cycle numbers up to 700 could be hardly distinguished from that of cycle number 500. The profile position of the latter can be considered the limiting position.

During desorption in bed 1, in the first half cycle, the favorable isotherm causes the concentration front to broaden. This broadening is enhanced due to the limiting mass transport from inside the adsorbent particles into the liquid phase. At the same time, $CoCl_2$ leaving the reactor enters bed 2 and is adsorbed in the unused part. Here the concentration difference between the liquid and solid phase is maximal, leading to the highest possible mass transfer and the concentration front remains straight.

When reversing the flow direction, $CoCl_2$ leaving the reactor now comes in contact with a partially preloaded volume of adsorbent in bed 1. Now the favorable isotherm causes the wave front to sharpen, but not to its full extent, due to a limiting uptake rate.

At the end of the first cycle, the penetration of the catalyst extends slightly to the left of its initial position in bed 1, shown at the left hand side in Figure 4A, but not to an extent that leaching may occur The model calculations show clearly that as more cycles have passed, the final position of the concentration front at the end of each subsequent cycle converges to a limiting value. This means that the metal catalyst is contained within the system.

The change of profile positions depicted in Figure 2 assumes the use of an adsorbent with relatively fast desorption and intermediate strength of adsorption. The calculated concentration profiles for the polymer-bound trifenylphosfine adsorbent in Figure 4 differ from the general picture presented in Figure 2. The parameters given in Table 1 correspond with the polymer-bound PPh_3 adsorbent that is shown[13] to adsorb $CoCl_2$ reversibly. This adsorbent is not the optimal one because of its slow desorption and its relatively strong adsorption; only a part of the columns is active in the adsorption–desorption cycles. Therefore, we studied the influence of adsorption strength, adsorption capacity, and diffusivity by changing the corresponding parameter values, one at a time. As shown in chapter 5 of ref. 14, the catalyst is still contained within the system boundaries at parameter values of at least a factor of two larger and smaller.

Conclusion

Calculation of $CoCl_2$ concentration profiles in polymer-bound trifenylfosfine adsorbent shows that after repeated adsorption/desorption cycles these profiles stabilize. Hence, the metal can be contained within the system, which is an essential requirement for the application of RFA.

Literature Cited

1. Dunnewijk J, Bosch H, De Haan AB. Reverse flow adsorption concept for the recovery of homogeneous catalysts: a technical feasibility study. *AIChE Meeting*, Reno NV, 2001.
2. Dunnewijk J, Bosch H, De Haan AB. Reverse flow adsorption: integrating the recovery and recycling of homogeneous catalysts. *Sep Pur Technol*. 2004;40:317–320.
3. Cotrell FG. Purifying gases and apparatus therefore. *U.S. Patent* 2,171,733, June 21, 1938.
4. Matros YSH, Bunimovich GA. Reverse-flow operation in fixed bed catalytic reactors. *Catal Rev—Sci Eng*. 1996;38:1–86.
5. Agar DW, Ruppel W. Multifunctionale Reaktoren fur die heterogene Katalyse. *Chem Ing. Tech*. 1998;60:731–741.
6. Noskov AS. Catalytic purification of gases from organic admixtures and nitrogen oxides in the region of a moving heat wave. *Combust Explosion Shock Waves*. 1997;33:284–293.
7. Snyder JD, Subramaniam B. Numerical simulation of a reverse-flow NO_x-SCR reactor with side-stream ammonia addition. *Chem Eng Sci*. 1998;53:727–734.
8. Beckmann A, Keil FJ. Increasing yield and operating time of SLP-catalyst processes by flow-reversal and instationary operation. *Chem Eng Sci*. 2003;58:841–847.
9. Björnbom P, Åkermark B. A catalytic process in a reverse flow reactor. *PCT Patent* Appl WO 01/28674, to KTH Holding AB, April 26, 2001.
10. Björnbom P, Hung KGW, Anderlund M, Åkermark B. Reverse flow operation for catalyst trapping. *AIChE Meeting*, Reno, NV, 2001.
11. Hung KGW, Anderlund M, Åkermark B, Björnbom P. A reverse flow reactor for homogeneous/heterogeneous catalysis. *AIChE Meeting*, Los Angeles CA, 2001.
12. Hung KGW, Papadias D, Björnbom P, Anderlund M, Åkermark B. Reverse-flow operation for application of imperfectly immobilzed catalysts. *AIChE J*. 2003;49:151–167.
13. Dunnewijk J, Bosch H, De Haan AB. Reverse flow adsorption technology for the recycling of homogeneous catalysts: Selection of suitable adsorbents. Proceedings of the 3rd Pacific Basin Conference on Adsorption Science and Technology, Kyongju, 2003:291–295.
14. Dunnewijk J. Reverse flow adsorption technology for homogeneous catalysts recycling, *PhD Thesis*, University of Twente, 2006.
15. Dunnewijk J, Bosch H, De Haan AB. Adsorption kinetics of $CoCl_2$ and PPh_3 over macroreticular and gel-type adsorbents by a generalized ZLC-method. *Chem Eng Sci*. 2005;61:4813–4826.
16. Wankat PC. *Separation Process Engineering*, *2nd ed*. Upper Saddle River: Prentice Hall, 2007.
17. Glückauf E, Coates JI. Theory of chromatography 4. The influence of incomplete equilibrium on the front boundary of chromatograms and on the effectiveness of separation. *J Chem Soc*. 1947;1315–1321.
18. Glückauf E. Theory of chromatography 10. Formulae for diffusion into spheres and their application to chromatography. *Trans Faraday Soc*. 1955;51:1540–1551.
19. McCue JT, Kemp G, Low D, Quinõnes-Garcia I. Evaluation of protein-A chromatography media. *Chromatogr A*. 2003;989:139–153.
20. Chung SF, Wen CY. Longitudinal dispersion of liquid flowing through fixed and fluidized beds. *AIChE J*. 1968;14:857–866.

Manuscript received May 15, 2007, and revision received Sept. 26, 2007.